Int. J. Electrochem. Sci., 15 **(2020)** 8108 – 8118, doi: 10.20964/2020.08.76

International Journal of
ELECTROCHEMICAL
SCIENCE
www.electrochemsci.org

Self-assembly of Amino-Functionalized MOF as Highly Dispersed Cathode Catalyst for Microbial Fuel Cells

Qiang Zhang[†1,2], *Xuedong Zhao*[†2], *Yunhua Hou*[2], *Xiaoliang Wang*[2], *Wenjie Li*[2], *Guangli Liu*[2], *Jingzhen Wang*[1,2,*], *Jing Yang*[3,*], *Qinzheng Yang*[1,2,*]

[1] State Key Laboratory of Biobased Material and Green Papermaking, Qilu University of Technology, Shandong Academy of Sciences, Jinan, 250353, Shandong, P. R. China
[2] Department of Bioengineering, Qilu University of Technology (Shandong Academy of Sciences), Jinan 250353, Shandong, P.R. China
[3] School of Electronic and Information Engineering (Department of Physics), Qilu University of Technology (Shandong Academy of Sciences), Jinan 250353, Shandong, P.R. China
[†] Qiang Zhang and Xuedong Zhao contributed equally
[*]E-mail: wjz_424@163.com, yangjing.xy@163.com, yqz@qlu.edu.cn

Received: 20 December 2019 / *Accepted:* 1 May 2020 / *Published:* 10 July 2020

The uniform dispersion of the catalyst is a key factor for the preparation of high-performance microbial fuel cell (MFC) cathodes. Herein, we self-assemble the amino ligand onto the surface of the carbon cloth (CC) by a one-pot method and complex the copper ions to form an amino-functionalized copper metal-organic framework (Cu-MOF-NH_2) as a cathode catalyst for the MFC. The positive charge and polarity of the amino group improve the interaction between the Cu-MOF-NH_2 and the carbon-based electrode, achieving high dispersion and high catalytic activity of the Cu-MOF-NH_2. The application results show that the Cu-NOF-NH_2 modified cathode provides a maximum power density of 0.64 Wm^{-2} for the MFC, which is 3.2 times higher than that of the CC base cathode. This work has explored a facile preparation method for a highly dispersed non-precious metal catalyst applied to a cathode, which has certain guiding significance for the large-scale popularization and application of MFCs.

Keywords: Cu-MOF-NH_2, Air cathode, MFC, Self-assembling, ORR

1. INTRODUCTION

MFC, as a new technology, can not only degrade and remove organic pollutants in wastewater but also generate electricity [1]. Among all kinds of MFCs, the single chamber microbial fuel cell (SCMFC) composed of air cathode can directly use the oxygen in the air as the electron acceptor, which is considered to be one of the most practical structures [2, 3]. Precious metals are commonly used as

catalysts in electrodes due to their excellent performance, but these precious metals are very expensive (e.g. $140/g for Pt), which limits the extensive application in MFCs [4]. Therefore, the research focus on cathode catalyst is transferring to non-precious metal catalytic materials to replace precious metal.

Metal-organic framework (MOF) is formed by metal cations and organic linkers, possessing advantages of adjustable structure and abundant metal sites, which is considered to be a promising non-precious metal catalytic oxygen reduction reaction (ORR) material for their potential application in electrocatalysis [5, 6]. However, the metal cations in the MOF are affected by the organic ligands, making the structure unstable and causing a decrease in catalytic efficiency [7-9]. High temperature Carbonization is a common method to increase the stability and catalytic activity of MOF [10, 11]. Recently, it has been found that MOF stability and catalytic activity can also be improved by adjusting the type of ligand or the combination of ligand and metal [12, 13]. These non-carbonized high catalytically active MOFs have been used in the fields of water decomposition, photocatalysis, electrochemical energy storage and MFCs [14-17]. Huang synthesized a nonpyrolyzed Fe-N coordination based MOF material and verified that it can effectively and stably catalyze the redox reaction [18]. Sohrabi designed a three-dimensional metal-organic framework graphene nanocomposite, which showed high catalytic performance in redox reaction [19]. Xue use zinc as metal cation and 2-methylimidazole as ligand to synthesize MOF and applied in air cathode [20].

Although MOF materials with good catalytic activity have been used as cathode catalysts in MFC, but the power density is still not ideal. In the process of preparing the air cathode, the agglomeration of MOF nanoparticles on the electrode substrate is caused by the existing manufacture methods, which effects the catalytic performance of the electrode. Therefore, it is necessary to optimize electrode preparation process and exploit the functionalized ligand with polarity or electrical to inhibit the potential agglomeration of metal sites for the fabrication of electrodes with highly dispersed and catalytically active MOF nanoparticles.

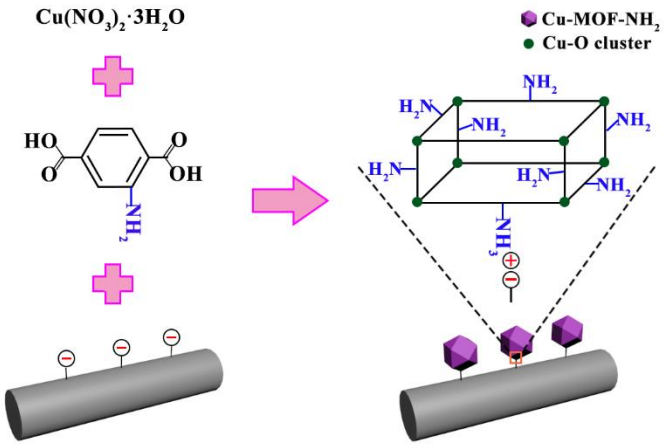

Figure 1. Schematic illustration of the synthesis and structure of Cu-MOF-NH_2.

Herein, we have developed a convenient one-pot method to prepare the efficient cathode with Cu-MOF-NH_2. Amino ligand was self-assembled onto the surface of the carbon substrate and then complex the copper ions (Fig. 1). The performance of Cu-MOF-NH_2 modified cathode was examined in both electrochemical tests and in MFCs tests. Meanwhile, the physical and chemical properties of Cu-MOF-NH_2 catalysts were studied by a series of characterization methods.

2. MATERIAL AND METHODS

2.1. Materials

MFC reactor purchased from Wente Co., Ltd (Jiangsu, China). Carbon cloth (CC, HCP330N), Carbon black (CB, VXC72R), Poly-tetrafluoroethylene (PTFE, 60 wt%) purchased from Hesen Co., Ltd (Shanghai, China). 2-Aminoterephthalic acid (2-NH_2-BDC) and p-Phthalic acid (H_2BDC) purchased from Macklin@ Co., Ltd (Shanghai, China). $Cu(NO_3)_2 \cdot 3H_2O$, Polyvinylpyrrolidone K30 (PVP), CTAB, N, N-Dimethylformamidel (DMF) purchased from Sinopharm Chemical Reagent Co., Ltd (Shanghai, China). In this experiment, all the reagents were analytical purity and used directly without any further purification.

2.2. Synthesis of catalyst

Modified CC with Cu-MOF-NH_2 as catalyst layer was prepared by one-pot method [21-23]. First, the CC (5×5 cm) was heat-treated in the mixture of nitric acid and sulfuric acid (v, 1:3) for 3 hours to form carboxyl group. Second, dissolved 1.2 g PVP in 24 ml DMF and 24 ml ethanol, which is solution Ⅰ. Solution Ⅱ is DMF (24 mL) contains $Cu(NO_3)_2 \cdot 3H_2O$ (0.6 mmol) and 2-NH_2-BDC (0.18 mmol). Mixed solution Ⅰ and solution Ⅱ, and ultrasonic treatment for 20 minutes to obtain the uniform solution which required for the preparation of MOF. Next, the mixed solution and CC were sealed in autoclave which contains PTFE tube, and kept 100℃ for 8 hours. After drop it to room temperature, ethanol and deionized water were used to wash the CC. The modified CC with Cu-MOF-NH_2 as catalyst layer was obtained by drying the CC in a vacuum freeze dryer at -50℃ for 12 hours, termed as CC/Cu-MOF-NH_2.

The modified CC with copper metal-organic framework (Cu-MOF) as catalyst layer was obtained by the same method. Replace the solution Ⅱ with Cu $(NO_3)_2 \cdot 3H_2O$ (0.9664 g, 4 mmol) and H_2BDC (0.6645 g, 4 mmol) and dissolved them in DMF (45 mL). It needed to be heated to 110℃ and kept for 21 hours in the autoclave. The CC was washed with DMF and ethanol, and then heated in vacuum at 100℃ for 12 hours to obtain the modified CC with Cu-MOF as catalyst layer, termed as CC/Cu-MOF.

2.3. Air-cathode preparation

All the cathodes were made up of three portions, the gas diffusion layer, catalyst layer and CC. The diffusion layer was in contact with air and the catalyst layer was exposed to solution. 30wt%

polytetrafluoroethylene solution which containing 20 uL/mg CB was coated on the air side of the CC, after dried the CC was calcined at 310℃ for 30 minutes to prepare the carbon base. Then, four layers of 60 wt% PTFE were prepared on the carbon base by the same

method, and finally the gas diffusion layer was formed [24, 25].

2.4. Physical and Electrochemical characterization

X-ray diffraction (XRD) analysis was used to characterize crystal structure and performed with a D8-ADVANCE X-ray diffractometer using Cu Kα source, the 2θ ranged from 5° to 30°. Fourier transform infrared (FT-IR) spectra were collected with a Nicolet10 spectrometer to analyze the material groups in the range of 600-4000 cm^{-1} with a resolution of 4 cm^{-1}. The Brunauer-Emmett-Teller (BET) specific surface area of material was based on N_2 adsorption-desorption curves with a gas adsorption analyzer (Geminiv2380) operating at 77 k with a relative pressure range 0.10-0.30. The contact angle of the material was obtained by a static water contact angle measuring instrument (KRUSS DSA100). The surface morphology of the prepared MOF nanoparticles was observed by scanning electron microscopy (SEM, HITACHI Regulus8220). Three electrode system of electrochemical workstation (Chenhua CHI604E) was used for electrochemical test. The catalyst electrode was the working electrode, the carbon rod electrode was the counter electrode, and the silver/silver chloride electrode was the reference electrode. The cyclic voltammetry (CV) was recorded in the range from -0.8 V to +0.8 V at the scan rate of 10 mV/s.

2.5. MFC construction and operation

MFC were designed in single chamber air cathode with a volume of 28.66 mL and inoculated with anaerobic activated sludge. The anode was made of CC and is treated with the same acid mixture as when the cathode CC is treated. The solution in air-cathode SCMFCs were comprised of 5 ml anaerobic activated sludge and 23.66 ml culture media. The culture media contained 1.36 mg/mL $CH_3COONa·3H_2O$, 0.11 mg/mL $CaCl_2$, 0.247 mg/mL $MgSO_4$, 3 mg/mL KH_2PO_4, 0.5 mg/mL NaCl, 1 mg/mL NH_4Cl, 17.8 g mg/mL $Na_2HPO_4·12H_2O$. The MFCs was operated at room temperature. A resistance (1000 Ω) was loaded between the anode and air-cathode during operation, and the output voltage was recorded by electrochemical collector. The CC cathode without catalyst was used as Control.

3. RESULTS AND DISCUSSION

3.1. Characterization of modified cathode

The structure characteristics of Cu-MOF and Cu-MOF-NH_2 were investigated by FTIR and XRD. Compared with Cu-MOF, the wide peak of Cu-MOF-NH_2 at 3500 cm^{-1} was due to the stretching vibration of amino group (Fig. 2a). This result proves that the amino group was successfully added to

the material [26, 27]. Hydrogen bonds can be established between the -NH_2 by ligand, and the small distance between the amino groups in Cu-MOF-NH_2 leads to weak hydrogen bonds in the amination material itself, thus forming wide peak instead of dispersive bands [28, 29]. It indicates that amino groups were regularly embedded in the MOF framework with a stable distance. Compared with Cu-MOF, after the amination of the ligand, the electrons on the benzene ring tend to the Cu II center, which causes the electrons to enrich to the Cu II center and cause polarization [30]. It is proved that the embedment of the amino group brings positive charge to the benzene ring and the MOF structure. The XRD patterns of Cu-MOF-NH_2 and Cu-MOF are similar, which shows that the skeleton structure will not be changed after amination (Fig. 2b).

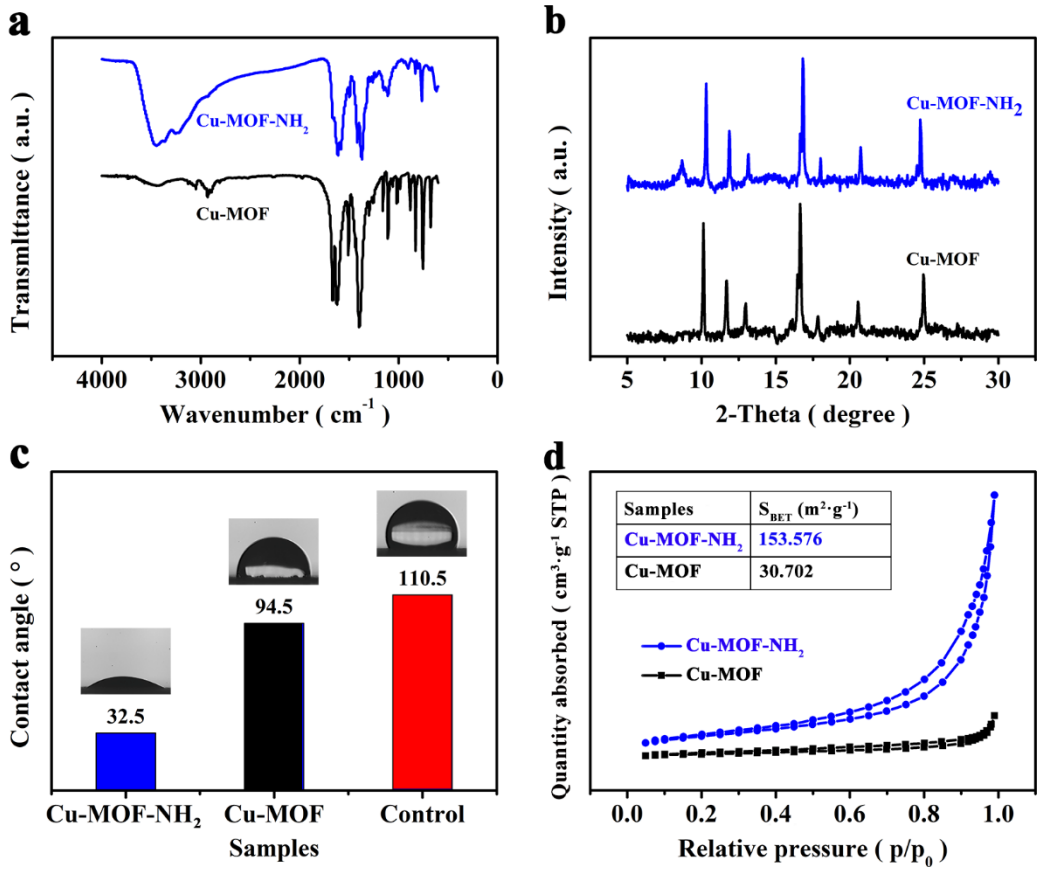

Figure 2. (a) FTIR spectra of Cu-MOF and Cu-MOF-NH_2, (b) XRD patterns of Cu-MOF and Cu-MOF-NH_2, (c) Surface contact angle of Control, CC/Cu-MOF and CC/Cu-MOF-NH_2, (d) N_2 adsorption/desorption isotherm of Cu-MOF and Cu-MOF-NH_2.

The major characteristic diffraction peaks of the two materials are concentrate in the range of 2θ=10-25° which is consistent with previous researches [21, 31]. After the incorporation of the -NH_2 group, the intensity of the diffraction peaks of MOF increased, which is attributed to the stronger complexing ability of aromatic -NH_2 with the metal center, resulting in higher crystallinity of Cu-MOF-NH_2 and more regular arrangement of internal molecules [27, 32]. This is consistent with the results of FTIR. At 2θ=10° (MOF characteristic peak) and 2θ=17.5° (main peak), the diffracted ray of Cu-MOF-

NH_2 is wider than that of Cu-MOF, indicating that Cu-MOF-NH_2 has a smaller crystal grain size. Amination increases the polarity force to make the crystal and water combine more evenly in the process of precipitation, not only leading to the minification and regular arrangement of the Cu-MOF-NH_2, but also makes it better to adsorb gas and transfer electron during ORR. The amino group changes the distribution of positive charge and polar force, promotes its uniform dispersion in the base electrode during the self-assembly process and increase the catalytic efficiency of the cathode in MFCs.

The electrodes surface characteristics were analyzed by static water contact angle tester and gas adsorption analyzer. The contact angles of CC and Cu-MOF assembly CC are 110.5° and 94.5° respectively, while the contact angles of Cu-MOF-NH_2 assembly CC are 32.5° (Fig. 2c). The hydrophobic surface of CC was not changed after Cu-MOF modification, while Cu-MOF-NH_2 increased the wettability of CC and the surface change to hydrophilic. These amino MOFs can be assembled with carboxyl groups on the surface of CC to form a uniform distribution. In the ORR of Air cathode, O_2 combines with protons and electrons in the electrode solution, and the final reaction site is liquid [33]. The cathode modified by Cu-MOF-NH_2 can improve the efficiency of ORR by changing the surface from hydrophobic to hydrophilic.

N_2 adsorption-desorption isothermal curves was used to test the investigate surface characteristics of different cathodes. In Fig. 2d, the cathodes with Cu-MOF and Cu-MOF-NH_2 have hysteresis loops which indicates the existence of mesoporous and micropores structure [34]. The presence of mesopores and micropores facilitates the transport of oxygen and electrolytes during ORR [7]. Compared Cu-MOF and Cu-MOF-NH_2 through BET technique，the latter has a larger surface area (153.576 $m^2 \cdot g^{-1}$) than the former. The amino group embedded around the Cu-MOF-NH_2 ligand changes the pore size and pore type, so the material possess larger porosity and specific surface area [35]. This structural optimization promotes the adsorption and transport of O_2 and improves the efficiency of ORR. In the application of air cathode, Cu-MOF-NH_2 catalyst layer can obtain higher ORR catalytic efficiency via good hydrophilicity and larger specific surface area, which further shows its excellent electrochemical performance.

3.2. Surface morphology of cathode

Morphological features of the different catalysts attached to CC were studied by electron microscopy techniques. In Fig. 3a, most of the Cu-MOF crystals are connected with the carbon cloth by being embedded in a narrow gap between the carbon fibers. However, Cu-MOF-NH_2 is uniformly and intensively covered on the surface of carbon fiber (Fig.3c). It is known that amino groups have been used to facilitate the connection of MOF with other materials. For example, Shen used chemisorption between the amino group on the ligand and the material to promote the connection of MOF to the material [36]. Therefore, the amino group on Cu-MOF-NH_2 can form chemical connection with the carboxyl group of carbon fiber which promotes the uniform dispersion and increases the adhesion. In Fig. 3b and 3d, the two cathode materials were compared by higher multiple images. The Cu-MOF crystal is a hexahedral structure with a size varying between 100 nm and 800 nm, while the Cu-MOF-NH_2 crystal is also a hexahedral structure with a size of about 50 nm. This shows that the size of the

crystal is reduced due to the repulsion of the amino charge force in the process of crystal precipitation after amino modification. Compared with Cu-MOF, Cu-MOF-NH_2 have more crystal units and expose more active sites on cathode, which can be considered as the reason for the improvement of electric efficiency in air cathode.

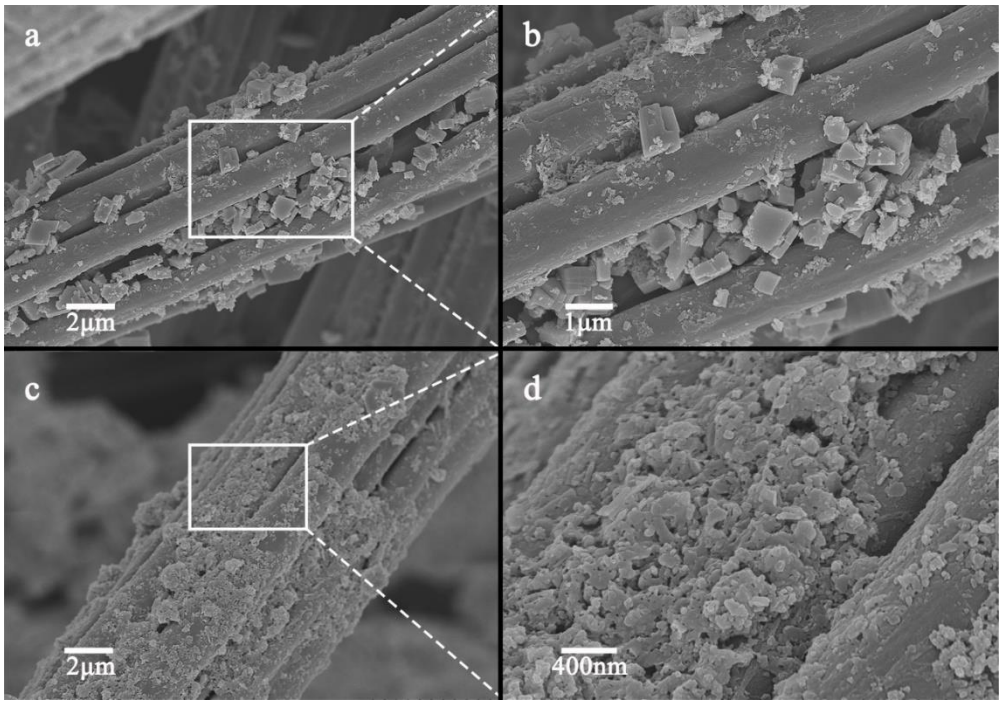

Figure 3. SEM images of CC/Cu-MOF (a and b) and CC/Cu-MOF-NH_2 (c and d).

3.3. Electrochemical characterization

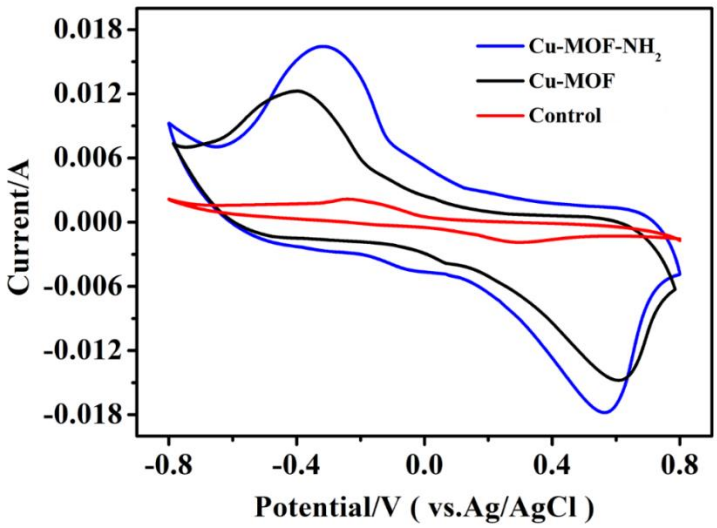

Figure 4. Cyclic voltammograms of Control electrode, Cu-MOF modified electrode and Cu-MOF-NH_2 modified electrode in PBS buffer at the scan rate of 10 mV/s.

CV usually consists of reverse scanning and forward scanning, which correspond to reduction reaction and oxidation reaction respectively [37]. The electrochemical activities of control electrode (bare CC), Cu-MOF modified electrode and Cu-MOF-NH_2 modified electrode were evaluated by CV (Fig. 4). In contrast to control electrode, which shows no distinctive redox peak in the scanned potential window, two redox peaks can be resolved in pure Cu-MOF modified electrode and Cu-MOF-NH_2 modified electrode, which are attributable to the redox reactions involving the Cu^{2+} center [38-41]. This indicates that the two materials can effectively catalyze the electrochemical reduction of oxygen at the cathode [13, 42]. Cu-MOF-NH_2 air cathode has the largest longitudinal extension current, the peak value of the reduction current is 0.16 A, and the value of the oxidation current is 0.17 A, which is significantly higher than that of Cu-MOF modified air cathode. At the same time, it was observed that the CV curve of the Cu-MOF-NH_2 modified cathode showed a larger electrochemically active area at the same potential compared to the other two cathodes, which means that Cu-MOF-NH_2 has a more stable three-dimensional structure and more exposed active centers [42, 43]. These results show that the excellent characteristics of Cu-MOF-NH_2 bring higher specific surface area, richer porous structure and more active sites for the electrode, which effectively promotes charge transfer on the electrode and improves ORR performance.

3.4. Electrochemical performance

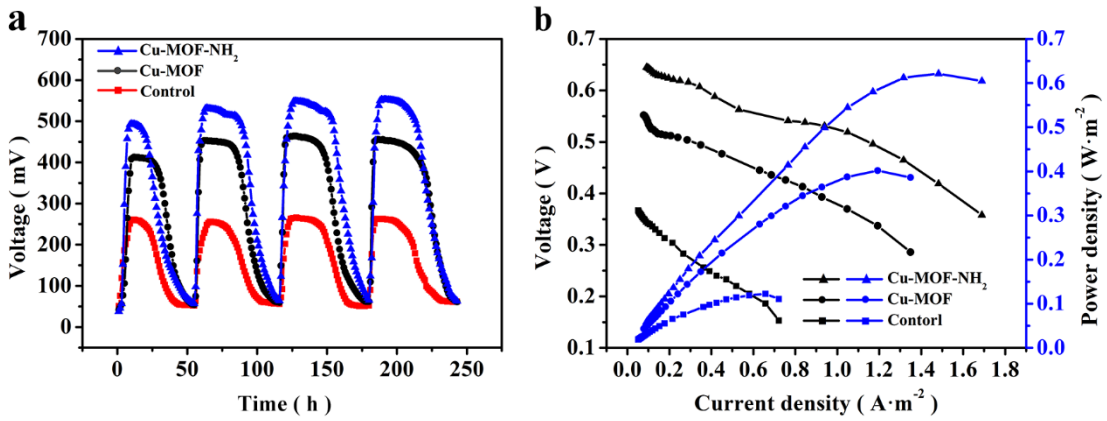

Figure 5. Voltage (a) and polarization curves (b) of MFCs with Control, CC/Cu-MOF and CC/Cu-MOF-NH_2 cathodes.

In order to verify the electricity production of the two cathode catalysts in MFC, the blank CC was used as a control. As shown in Fig. 5a, after four cycles operation, the electricity generation performance of three different air cathodes is significantly different. The output voltage (550 mV) of Cu-MOF-NH_2 modified air cathode is much higher than that of Cu-MOF (450 mV) and control (250 mV). The higher voltage platform implies a faster consumption of carbon source, demonstrating that the ORR performed on the air cathode is more efficient [44, 45], which is related to the excellent ORR catalytic activity of Cu-MOF-NH_2. It is worth noting that the highest voltage of Cu-MOF-NH_2 was maintained for 5 h in the first operation cycle, and the stable operation time reached 20 h in four operation

cycle, which indicates that the air cathode modified by Cu-MOF-NH_2 is stable in operation. At the same time, it can be observed that in the fourth round, the voltage stability of each MFC has slightly decreased. This is due to the deposition of salts on the solution side of the cathode, which reduces the conductivity of the cathode. Precipitation of phosphate in the culture medium can potentially reduce cathode performance by affecting the conductivity of the catalyst [46].

Table 1. Performance comparison of MOF and other materials.

materials	power density
Cu-MOF-NH_2	0.64 Wm^{-2}
Co-N-C	0.399±0.01 Wm^{-2}
Fe-N-C/AC	0.73±0.01 Wm^{-2}
Cu-bipy-BTC-derived	0.349±0.012 Wm^{-2}
Pt	0.766 Wm^{-2}
3D biofilm	0.843±0.031 Wm^{-2}

The Polarization curve is another common method to evaluate the performance of MFC by changing the external load resistance, which is usually obtained by steadily decreasing the external resistance when the steady voltage is reached [47]. In Fig. 5b, it is found that the maximum power density (0.64 Wm^{-2}) of Cu-MOF-NH_2 is 3.2 times and 1.4 times higher than that of control (0.20 Wm^{-2}) and Cu-MOF (0.45 Wm^{-2}) respectively when the current density is 1.5 Am^{-2}. The excellent battery performance is also in accordance with the result of voltage diagram. We compared some similar catalyst materials in Table 1. The maximum power density of Cu-MOF-NH_2 is higher than or close to some MOF catalysts used in air cathodes without precious metals, such as Co-N-C electrodes (0.399±0.01 Wm^{-2}) [42], Fe-N-C/AC electrodes (0.73±0.01 Wm^{-2}) [48], Cu-bipy-BTC-derived electrode (0.349±0.012 Wm^{-2}) [49]. The maximum power density of Pt as the cathode catalyst is 0.766 Wm^{-2} [24], which is 15% higher than that of Cu-MOF-NH_2 catalyst, but the price of Cu-MOF-NH_2 is lower than Pt. Compared with other 3D network materials, such as 3D biofilm (0.843±0.031 Wm^{-2}) [50], Cu-MOF-NH_2 also shows good performance. The above results show that the polarity of Cu-MOF-NH_2 tends to be consistent after amino functionalization. Amino groups bring high specific surface area, stable structure and exposed active sites to MOF. These characteristics increases the electron transfer speed of cathode and enhances the uniform distribution of MOF to form more uniform active sites which can promote the ORR catalytic efficiency and the electrical performance.

4. CONCLUSION

In summary, the Cu-MOF-NH_2 was uniformly assembled on the cathode by one-pot method, and verified its performance in MFCs. The ligand with amino group changed the charge force and polarity force of Cu-MOF, increased the dispersion and surface area of Cu-MOF, which made it more evenly distributed on the CC substrate and had better catalytic activity compared with ordinary Cu-MOF. The

maximum power density produced by MFC with Cu-MOF-NH_2 as the cathode catalyst is 0.64 Wm^{-2}, which is significantly higher than the maximum power density produced by MFC with ordinary Cu-MOF as the cathode catalyst, which reflects better electrochemical performance. This study provides a simple method to prepare modified MOF as a high efficiency ORR catalyst, which has great significance for the development of high-performance MFCs cathode materials.

ACKNOWLEDGEMENT
The authors are grateful for the financial support from the National Natural Science Foundation of China (Grant No. 31800116), Natural Science Foundation of Shandong Province, China (Grant No. ZR2018LC004).

References

1. C. Santoro, R. Gokhale, B. Mecheri, A. D'Epifanio, S. Licoccia, A. Serov, K. Artyushkova and P. Atanassov, *ChemSusChem*, 10 (2017) 3243.
2. X. Zhang, K. Li, P. Yan, Z. Liu and L. Pu, *Bioresour. Technol.*, 187 (2015) 299.
3. E. Zhang, F. Wang, Q. Yu, K. Scott, X. Wang and G. Diao, *J. Power Sources*, 360 (2017) 21.
4. B. Wei, J.C. Tokash, G. Chen, M.A. Hickner and B.E. Logan, *RSC Adv.*, 2012, 2, 12751.
5. A. Corma, H. Garcia and F.X. Llabres i Xamena, *Chem. Rev.*, 110 (2010) 4606.
6. X.F. Lu, P.Q. Liao, J.W. Wang, J.X. Wu, X.W. Chen, C.T. He, J.P. Zhang, G.R. Li and X.M. Chen, *J. Am. Chem. Soc.*, 138 (2016) 8336.
7. H. Zhong, K.H. Ly, M. Wang, Y. Krupskaya, X. Han, J. Zhang, J. Zhang, V. Kataev, B. Buchner, I.M. Weidinger, S. Kaskel, P. Liu, M. Chen, R. Dong and X. Feng, *Angew. Chem. Int. Ed.*, 58 (2019) 10677.
8. L. Sun, M.G. Campbell and M. Dinca, *Angew. Chem. Int. Ed.*, 55 (2016) 3566.
9. E.M. Miner, T. Fukushima, D. Sheberla, L. Sun, Y. Surendranath and M. Dinca, *Nat. Commun.*, 7 (2016) 10942.
10. S. You, X. Gong, W. Wang, D. Qi, X. Wang, X. Chen and N. Ren, *Adv. Energy Mater.*, 6 (2016) 1501497.
11. H. Tang, S. Cai, S. Xie, Z. Wang, Y. Tong, M. Pan and X. Lu, *Adv. Sci.*, 3 (2016) 1500265.
12. G. Chen, J. Zhang, F. Wang, L. Wang, Z. Liao, E. Zschech, K. Mullen and X. Feng, *Chem. Eur. J.*, 24 (2018) 18413.
13. J. Mao, L. Yang, P. Yu, X. Wei and L. Mao, *Electrochem. Commun.*, 19 (2012) 29.
14. P. Tian, D. Liu, K. Li, T. Yang, J. Wang, Y. Liu and S. Zhang, *Bioresour. Technol.*, 244 (2017) 206.
15. Y.C. Zhou, W.W. Dong, M.Y. Jiang, Y.P. Wu, D.S. Li, Z.F. Tian and J. Zhao, *J. Solid State Chem.*, 279 (2019) 120929.
16. G.B. Xiao, X.Q. Yao, H. Xie, H.C. Ma, P.J. Yan and D.D. Qin, *Polyhedron*, 162 (2019) 39.
17. Y.S. Li, J.W. Yi, J.H. Wei, Y.P. Wu, B. Li, S. Liu, C. Jiang, H.G. Yu and D.S. Li, *J. Solid State Chem.*, 281 (2020) 121052.
18. Z.H. Huang, N.H. Xie, M. Zhang and B.Q. Xu, *ChemSusChem*, 12 (2019) 200.
19. S. Sohrabi, S. Dehghanpour and M. Ghalkhani, *ChemCatChem*, 8 (2016) 2356.
20. W. Xue, Q. Zhou, F. Li and B.S. Ondon, *J. Power Sources*, 423 (2019) 9.
21. Z. Yao, Z. Li, H. Liu, Y. Liu, Y. Sun and Z. Li, *Anal. Methods*, 11 (2019) 1697.
22. Q. Huang, P. Zhou, H. Yang, L. Zhu and H. Wu, *Electrochim. Acta*, 232 (2017) 339.
23. L. Peng, X. Gong, X. Wang, Z. Yang and Y. Liu, *RSC Adv.*, 8 (2018) 26377.
24. S. Cheng, H. Liu and B.E. Logan, *Electrochem. Commun.*, 8 (2006) 489.
25. E. Antolini, R.R. Passos and E.A. Ticianelli, *J. Appl. Electrochem.*, 32 (2002) 383.

26. S. Wang, W. Deng, L. Yang, Y. Tan, Q. Xie and S. Yao, *ACS Appl. Mater. Interfaces*, 9 (2017) 24440.
27. J. Gascon, U. Aktay, M. Hernandezalonso, G. Vanklink and F. Kapteijn, *J. Catal.*, 261 (2009) 75.
28. X. Kong, H. Deng, F. Yan, J. Kim, J.A. Swisher, B. Smit, O.M. Yaghi and J.A. Reimer, *Science*, 341 (2013) 882.
29. Z.H. Rada, H.R. Abid, H. Sun, J. Shang, J. Li, Y. He, S. Liu and S. Wang, *Prog. Nat. Sci.*, 28 (2018) 160.
30. L. Li, S. Zhu, R. Hao, J.J. Wang, E.C. Yang and X.J. Zhao, *Dalton Trans.*, 47 (2018) 12726.
31. G.H. Dang, Y.T.H. Vu, Q.A. Dong, D.T. Le, T. Truong and N.T.S. Phan, *Appl. Catal., A*, 491 (2015) 189.
32. C. Liu, Y. Wang, Y. Zhang, R. Li, W. Meng, Z. Song, F. Qi, B. Xu, W. Chu, D. Yuan and B. Yu, *Chem. Eng. J.*, 354 (2018) 835.
33. B.E. Logan and K. Rabaey, *science*, 337 (2012) 686.
34. M. Kruk and M. Jaroniec, *Chem. Mater.*, 13 (2001) 3169.
35. F. Luo, M.S. Wang, M.B. Luo, G.M. Sun, Y.M. Song, P.X. Li and G.C. Guo, *Chem. Commun.*, 48 (2012) 5989.
36. W.J. Shen, Y. Zhuo, Y.Q. Chai and R. Yuan, *Anal. Chem.*, 87 (2015) 11345.
37. Y. Lu, N. Zhu, F. Yin, T. Yang, P. Wu, Z. Dang, M. Liu and X. Wei, *Biosens. Bioelectron.*, 98 (2017) 350.
38. H. Chen, L. Wang, J. Yang and R.T. Yang, *J. Phys. Chem. C*, 117 (2013) 7565.
39. M. Jahan, Z. Liu and K.P. Loh, *Adv. Funct. Mater.*, 23 (2013) 5363.
40. R. Senthil Kumar, S. Senthil Kumar and M. Anbu Kulandainathan, *Microporous Mesoporous Mater.*, 168 (2013) 57.
41. W. Xia, A. Mahmood, R. Zou and Q. Xu, *Energy Environ. Sci.*, 8 (2015) 1837.
42. J.C. Li, X.T. Wu, L.J. Chen, N. Li and Z.Q. Liu, *Energy*, 156 (2018) 95.
43. X. Zheng, Y. Cao, D. Liu, M. Cai, J. Ding, X. Liu, J. Wang, W. Hu and C. Zhong, *ACS Appl. Mater. Interfaces*, 11 (2019) 15662.
44. C. Cao, L. Wei, M. Su, G. Wang and J. Shen, *J. Mater. Chem. A*, 4 (2016) 9303.
45. B. Li, Z. He, M. Wang and X. Wang, *Int. J. Hydrogen Energy*, 42 (2017) 5261.
46. J. Winfield, I. Ieropoulos, J. Greenman and J. Dennis, *Bioprocess. Biosyst. Eng.*, 34 (2011) 477.
47. J. Chen, Y. Hu, X. Tan, L. Zhang, W. Huang and J. Sun, *Bioresour. Technol.*, 241 (2017) 735.
48. R. Rossi, W. Yang, L. Setti and B.E. Logan, *Bioresour. Technol.*, 233 (2017) 399.
49. L. Zhang, Y. Hu, J. Chen, W. Huang, J. Cheng and Y. Chen, *J. Power Sources*, 384 (2018) 98.
50. Y.C. Yong, Y.Y. Yu, X. Zhang and H. Song, *Angew. Chem. Int. Ed.*, 53 (2014) 4480.